GEOLOCATION OF DEVICES USING LOW-POWER WIDE-AREA LORA NETWORK

Ladislav Zemko[*], *Daniel Hroš, Alexander Valach, Marek Galinski, Pavel Čičák*

Institute of Computer Engineering and Applied Informatics, Faculty of Informatics and Information Technologies, Slovak University of Technology, Ilkovicova 2, 842 16 Bratislava, Slovakia
[*]E-mail of corresponding author: ladislav.zemko@stuba.sk

Authors´ORCID IDs:
Ladislav Zemko - 0000-0002-5635-265X
Daniel Hroš - 0009-0002-7850-7509
Alexander Valach - 0000-0001-8299-0914
Marek Galinski - 0000-0001-6622-526X
Pavel Čičák - 0000-0002-3021-1971

Abstract: This article focuses on the geolocation possibilities in the context of the Internet of Things (IoT) and Low-Power Wide-Area Networks (LPWANs). A novel Logarithmic Distance Path Loss Model with a Memory (LDPL-M) algorithm to enhance the accuracy of determining the location of end devices based on trilateration using a Received Signal Strength Indicator (RSSI) is proposed. This technique proved to be more accurate by 25.54% compared to the conventional Logarithmic Distance Path Loss Model (LDPL), while focusing on low power consumption. Overall, the article provides valuable insight into the geolocation of LoRa end devices and highlights the importance of accurate and efficient geolocation methods in IoT and LPWANs applications.

Keywords: LoRa, LoRaWAN, geolocation, IoT, LPWAN, RSSI, trilateration

1 Introduction

LoRa technology belongs to the field of LPWANs. It enables the connection of a large number of end devices that send small volumes of data over long distances several times a day with minimal energy consumption. The devices last 5 to 10 years on a single charge and can be placed even in hard-to-reach places without access to electricity. The properties of LPWANs definitely enable device geolocation while maintaining low power consumption [1- 4]. LoRa is a wireless technology promoted by the LoRa Alliance. It utilizes a proprietary Chirp Spread Spectrum (CSS) modulation, which means a regular change in signal frequency - increasing or decreasing over time. It operates on the physical layer of the OSI model [2, 5]. It uses the freely available Industrial Scientific and Medical Band (ISM) for data transmission, so observing the so-called duty cycle (DC) is necessary. DC limits the time a device can transmit. Generally, this is 1% of the time, which equals 36 seconds per hour [6, 7].

Above the LoRa physical modulation operates the LoRaWAN protocol, ensuring bi-directional communication. LoRaWAN is standardized by the LoRa Alliance organization and has the possibility of roaming, but with the cost of higher energy consumption compared to other protocols, e.g., LoRa@FIIT developed at FIIT STU [6, 8, 9, 10]. A typical implementation of a LoRaWAN network consists of end devices (typically a simple battery-powered sensor), gateways, a network server, and an application server. In most applications, end devices are autonomous, connected in a star[1] topology, and send the collected data via LoRa technology to

[1] star-of-stars, respectively

all gateways within their range. After the gateway receives a message, it immediately adds metadata to it: timestamp, Received Signal Strength Indicator (RSSI), Signal to Noise ratio (SNR), and others, which are crucial in determining the location of the end device in wireless networks [8].

Our research focuses on the LoRaWAN protocol and the LoRa technology in general, which belong to the category of LPWANs. The accuracy of determining the location of end devices in LoRa networks depends on types of devices and communication parameters, as well as the geolocation method used, i.e. triangulation, trilateration, and multilateration. In this article, we deal with the method of trilateration based on the Received Signal Strength Indicator (RSSI). In this work we focus on the opportunities for the geolocation of end devices, particularly in connection with Low-Power Wide-Area Network (LPWAN), a wireless wide-area network with low energy consumption. Compared to standard methods of geolocation using global navigation systems (GNSS), LPWANs allow to determine the location of end devices over a relatively wide area with minimal power consumption. We proposed a novel logarithmic distance path loss model with memory (LDPL-M) algorithm, which takes into consideration not only the actual end device's location, but also previous locations. Results showed this modification improves the overall geolocation accuracy for non-stationary as well as stationary end devices.

The main contribution of this article lies in the following:

- Research in the field of LPWANs and suitable geolocation methods: The paper describes LPWANs with the focus on the LoRa technology and provides an overview of the methods applicable for the purposes LoRa end devices geolocation with low power consumption in mind.
- Proposal of the LDPL-M algorithm: A logarithmic distance path loss model with memory (LDPL-M) algorithm for the geolocation of end devices based on the trilateration using RSSI value is proposed. Compared to the existing solutions the algorithm computes the end device position using not only the actual location, but considers n previously determined locations, which improves the overall accuracy. The accuracy, or the error, respectively, of the proposed algorithm is also measured and compared to other methods, including GPS sensor data.

The article is organized as follows: Section 2 describes related work and provides basic information about LoRa technology and the LoRaWAN protocol. Additionally, this section describes the geolocation techniques applicable to these networks. Section 3 explains the methodology of building the private LoRaWAN network as well as data collection and processing in both the private and Slovanet provider networks. It also describes a method for estimating the initial position of the end device and proposes an LDPL-M algorithm to improve the accuracy of existing solutions depending on specific use cases. This section compares the accuracy of estimating the end device's location using different algorithms and describes the method of displaying this position on the map. Additionally, the impact on the end device's power consumption utilizing the GPS sensor was assessed. The gathered dataset is described in Section 4. Finally, Section 5 concludes the paper.

2 Related Work

Determining the location of LoRa end devices is an active research area, with several proposed methods and algorithms to enhance the overall accuracy. Recent studies have demonstrated that machine learning algorithms and hybrid methods combining different techniques offer promising results [5]. Furthermore, the deployment of LoRa gateways and proper positioning can significantly influence geolocation accuracy, so further research is still required to optimize gateway placement in different environments. Several studies have examined the deployment and type of LoRa gateways and their influence on geolocation accuracy, including a study [11] that examined the impact on geolocation accuracy in an urban environment.

Although considerable research has been done on geolocation in LoRa networks, there is a need for more publicly available data on this topic in Bratislava, Slovakia. Our study aimed to examine the accuracy and feasibility of geolocation in a real-world environment and provide insights into the factors that could impact the precision of location estimation.

The three most common techniques used for the geolocation of devices in a wireless network are multilateration, trilateration, and triangulation, which require knowledge of the location of reference points (gateways). The choice of the appropriate technique depends on the use case and the available information about the end device [12].

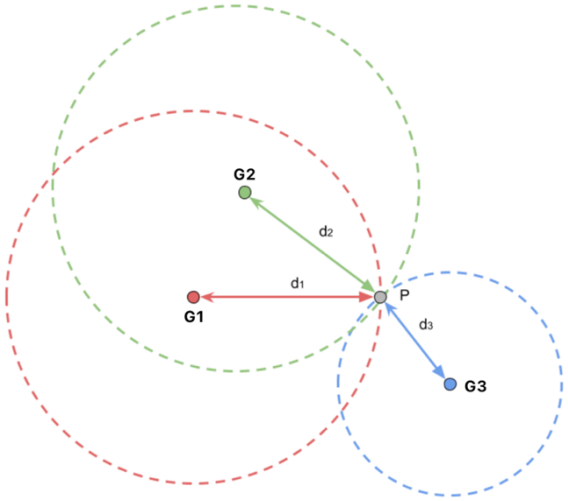

Figure 1 *Position calculation using trilateration [13]*

The trilateration method uses the distance between the transmitting device and each reference point in its calculation, as shown in Figure 1. The distance between devices can be calculated in two ways:

1. Based on the Time of Arrival (ToA),
2. Based on RSSI value.

For the correct calculation of the distance in the ToA method, it is essential to correctly determine the transmission time between devices. The proper determination of the transmission time requires time synchronization between the end device and all reference points in the network. Time synchronization on end devices requires additional communication and thus can increase power consumption. Trilateration using ToA for determining the end device's location is therefore unsuitable for LPWANs [12, 14].

The multilateration method does not require knowledge of the device's distance from each reference point as in the case of trilateration, but only the difference of distances from each reference point to the device. The time difference of arrival (TDoA) between the end device

and the reference points is used to calculate the distance difference. Thus, this method requires time synchronization only between reference points [12]. Even a small error in the time synchronization (1 μs) of the reference points can cause a significant error in determining the position of the end device (300 m) [15].

The triangulation method uses the geometry of a triangle defined by two angles of the signal angle of arrival (AoA) for calculation. However, AoA measurements are not suitable for determining the location of a device in a LoRa network due to the accumulating angle error with increasing distance of the device from the reference points [12].

In LPWANs, the methods of multilateration (TDoA values can be determined) and trilateration (RSSI value available in LoRaWAN packet) can be used to calculate the position of the end device. Studies show better accuracy of TDoA over RSSI [12, 16]. However, as the gateway clocks in our network are synchronized using Network Time Protocol (NTP) servers, we only achieved precision at milliseconds, which is not sufficient for geolocation based on the TDoA.

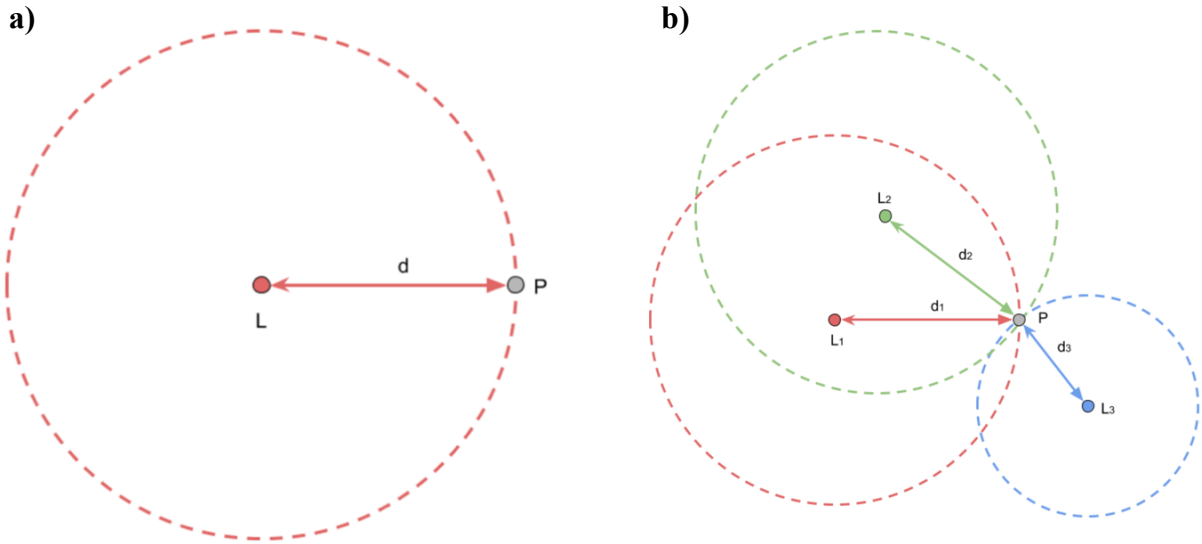

Figure 2 *Representation of distance from (a) single reference point and (b) multiple reference points [13]*

The trilateration method can be used to estimate end devices' location using RSSI. To simplify the calculations, the intersection of circles is in the Cartesian plane. Referring to Figure 2, we want to determine the device's *P* location using a reference point *L* whose location is known. Based on one reference point, we cannot determine the location of the device *P*, but we can estimate the distance *d* between *P* and *L* using techniques based on RSSI, as shown in Figure 2a. Each point is a potential candidate for *P* at this distance. For the correct determination of *P*, we need at least three circles whose intersection is at single point. This point represents the actual location of the device, shown in Figure 2b. We create multiple circles using various reference points, each at a known location L_i. For each reference point, we can determine the distance d_i from *P* [13]. The equation for a circle in a plane:

$$(x - c_x)^2 + \left(y - c_y\right)^2 = d^2, \tag{1}$$

where the point (x, y) on the Cartesian plane lies on a circle of radius *d* centered on (c_x, c_y). From (1), we can derive the equations for the circles generated by the reference points. Each reference point has a known location expressed by latitude and longitude coordinates (ϕ_i, λ_i).

We obtain the intersection of the circles by solving the system of three linear equations, thereby determining the location of the point $P = (\phi, \lambda)$ [13, 17]:

$$\begin{aligned} (\phi - \phi_1)^2 + (\lambda - \lambda_1)^2 &= d_1^2, \\ (\phi - \phi_2)^2 + (\lambda - \lambda_2)^2 &= d_2^2, \\ (\phi - \phi_3)^2 + (\lambda - \lambda_3)^2 &= d_3^2. \end{aligned} \tag{2}$$

This method is mathematically correct, but we encountered several problems that make it impractical. In the real world, a set of equations may not have a solution, as the circles may not intersect at a single point due to measurement error. For example, in [18], the authors tried to create a prototype of a wireless network in a coal mine, which could be used to navigate miners out of the mine in case of an emergency. However, the geolocation proved to be unsuccessful due to the significant interference of the environment, which caused errors in the measurement of the distances of the end devices from the reference points. In the same way, we cannot use measurements from more than three reference points in the analytical approach. Therefore, we approach this problem more like an optimization problem and search for a point $X = (\phi_x, \lambda_x)$ that provides the best approximation to P. Using the Mean Squared Error (MSE) calculation, we can verify how well the point X replaces the point P [18]:

$$\frac{\sum_{i=1}^{n}[d_i - dist(X, L_i)]^2}{n}, \tag{3}$$

where: $dist(X, L_i)$ is a distance between point X and reference point L_i.

If this distance coincides with the corresponding distance d_i, it contributes minimal error to the total error, or none at all (we assume that X is indeed P). The use of squares eliminates the mutual subtraction of positive and negative errors. The optimization algorithm should be able to converge to a reasonable result. However, by providing an estimate of the initial position of X, we can speed up its execution. The advantage is the possibility to use any number of reference points [13].

3 Proposed Solution

This section describes a novel LDPL-M algorithm for determining the end devices' location, including architecture, data collection and processing, initial position estimation, the LDPL-M algorithm itself, and results achieved so far for stationary and non-stationary devices. The requirements for the proposed technique and its evaluation were the following:

1. The geolocation of end devices powered by a limited power source. Geolocation is based on the trilateration method utilizing the RSSI in a LoRaWAN network.
2. Comparison of the accuracy of existing geolocation methods within the trilateration. To compare the accuracy of individual geolocation techniques, a graph of the Cumulative Distribution Function (CDF) and a table of error rates of particular methods are used in each percentile. At the same time, using different methods depending on specific use cases may require different levels of accuracy.
3. Verification of the LDPL-M accuracy. An external GPS sensor is utilized to provide a reference value for the actual location of the end device, with an accuracy of 1.5 cm.
4. Visualization of the end devices' location on the map. As part of our work, a web interface that displays the last recorded location of the end device, along with information about the time of the most recent location update, was created.

5. Contribution to future research and community. This work also tries to contribute to the field of LPWANs and geolocation, respectively, by creating a publicly available dataset for the future continuation of research.

In our work, we focus on geolocation of the end device exclusively by the trilateration method based on the RSSI, as we were limited by the hardware capabilities. The basic principle of determining the end device's location based on RSSI consists of associating the path loss with the distance between the transmitted and received signal. Path loss represents the loss of signal strength that occurs during transmission through a communication medium and obstacles, such as air or a wall, respectively. Path loss can be calculated using the link budget, which includes all signal gains and losses during transmission from the transmitter to the receiver. This budget is defined by (4) [19, 20]:

$$P_{Rx} = P_{Tx} + G_{Rx} + G_{Tx} - L_{PL}, \tag{4}$$

where: P_{Rx} is a signal strength at the receiver,
P_{Tx} is a signal strength at the transmitter,
G_{Rx} is a gain of the antenna used by the receiver,
G_{Tx} is a gain of the antenna used by the transmitter,
L_{PL} is a path loss.

Path loss is calculated by substituting the RSSI value into P_{Rx} in (4). We can subsequently associate the path loss with the distance the signal has traveled through several models:

1. Free-space Path Loss Model (FSPL): The main idea is that the strength of a received wireless signal passing through free space decreases quadratically with increasing distance from the sender [21]:

$$P_{Rx}(d) = \frac{P_{Tx}G_{Tx}G_{Rx}\lambda^2}{(4\pi d)^2}, \tag{5}$$

where: $P_{Rx}(d)$ is a signal strength at receiver at distance d,
λ is a wavelength,
d is a distance between receiver and sender.

A more appropriate notation of such a model is in units of decibels (*dB*):

$$FSPL(d) = 20log_{10}(d) + 20log_{10}(f) + 20log_{10}(\frac{4\pi}{c}), \tag{6}$$

where: $FSPL(d)$ is a path loss at distance d,
d is a distance between receiver and sender,
f is a carrier frequency,
c is a speed of light.

2. Logarithmic Distance Path Loss Model (LDPL): In reality, the vast majority of signals are received in an environment without direct visibility of devices (Non-Line of Sight, NLoS), which results in interference, especially in built-up areas. Interference is caused by reflections from buildings, weather, and other variables,

considering utilization of FSPL more an idealization. Based on empirical evidence, it is more appropriate to estimate the distance according to the LDPL formula [14, 20]:

$$L_{PL}(d) = L_{PL}(d_0) + 10\beta log(\frac{d}{d_0}) + X_\sigma, \quad (7)$$

where: $L_{PL}(d)$ is a path loss at distance d in *dB,*
$L_{PL}(d_0)$ is a path loss at reference distance d_0 in *dB,*
β is a path loss exponent - an empirical constant dependent on the environment,
X_σ is a path loss random variable from the shading factor with zero Gaussian mean value and standard deviation σ in *dB*.

By substituting L_{PL} from (4) into (7), the distance d can be estimated if we have the values of the parameters β and $L_{PL}(d_0)$. These values can be obtained by performing empirical measurements - machine learning methods by fitting a logarithmic curve are used to describe best the data obtained by the measurements. The values of the parameters β and $L_{PL}(d_0)$ are dependent on the environment [22].

In addition to the mentioned models, there are other models such as Okumura-Hata, Cost 231, or IMT-2000 [20].

To improve the results of device geolocation using methods based on RSSI, Estimated Signal Power (ESP) is used, which represents the RSSI value with environmental interference considered. ESP is beneficial due to the characteristics of LoRa networks, in which devices can receive a relatively noisy signal (in practice, the gateway manages to decode even frames with an RSSI of approximately −120 dBm) [23]. We can write the ESP equation in the logarithmic form [20, 24]:

$$ESP_{(dBm)} = RSSI_{dBm} + SNR_{(dB)} - 10log_{10}(1 + 10^{0.1\,SNR_{(dB)}}). \quad (8)$$

We can continue to work with ESP in the same way as with RSSI, and therefore substitute it into P_{Rx} in (4) and then calculate the distance between the end device and the gateway using (7). For most of the previous works, which determined the position of the RSSI device, determining the position in a smaller area or sparsely built-up areas with minimal environmental interference was specific. Any environmental obstacle seriously affects the geolocation accuracy [20]. We therefore conclude that such device geolocation is more suitable for a smaller area and in an environment with direct visibility of devices (Direct Line of Sight, DLoS).

3.1 Architecture

In this section, the primary focus is on the architecture of the private LoRaWAN network. Unfortunately, we cannot access the architecture of the public provider network, so it cannot be discussed in more detail. Figure 3 shows the gateway locations within the private network. All gateways were strategically placed to form a polygon and maintain DLoS with the end device. The highlighted polygon illustrates the area in which the end device was able to move during the data collection. The network comprised the following components:

- End device: Development Kit LilyGo TTGO ESP32 with SX1276 LoRa Chip and built-in NEO-6M GPS module. The device was programmed to periodically transmit uplink (from the end device to the network server) messages at 868 MHz frequency band. The LMIC-node library [25] was used.

- Network server: Messages sent from end devices received by gateways were sent over the Internet to the ChirpStack network server. This open-source LoRaWAN network server provided a web interface to manage gateways, end devices, and applications [26]. Using the ChirpStack network server, we downloaded all measured data in JavaScript Object Notation (JSON) format, which was then processed to determine the geolocation of end devices.
- Gateways: During the data collection phase, we utilized 8 Raspberry Pi microcomputers as gateways within the network. These microcomputers were attached a compatible backplane connecting the Raspberry Pi to an iC880A LoRaWAN concentrator with an 868 MHz antenna. Each Raspberry Pi gateway was running the Raspberry Pi OS operating system. One of the key advantages of using Raspberry Pi gateways was their mobility, as power banks could power them. This enabled us to position the gateways in any location necessary to optimize the data collection process.

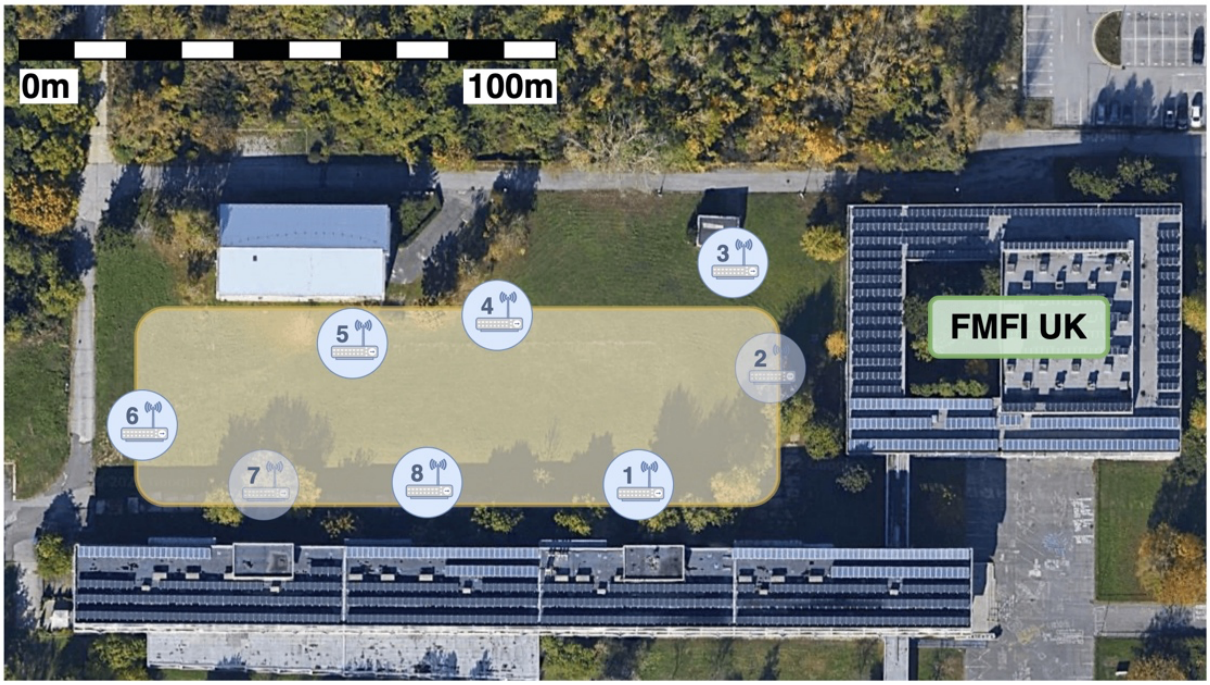

Figure 3 *Gateways position - Google Maps data*

A microservice architecture shown in Figure 4 was utilized during the data collection and experiments. It consists of the following services:

- Hypertext Transfer Protocol (HTTP) Server: A minimalist HTTP server based on the Python. The ChirpStack network server allows captured uplink messages from the end device to be sent in real time to any Internet Protocol (IP) address using the HTTP protocol. The task of the HTTP server is to capture messages from the ChirpStack network server and then forward them via the HTTP protocol to a Geolocation Solver service.
- Message Queuing Telemetry Transport (MQTT) Client: A simple MQTT subscriber. The public provider sends real-time uplink messages from the end device to this topic. When implementing the subscriber, we suggest using the paho.mqtt Python module.

The task of this service is similar to the previous case, i.e., to forward uplink messages to Geolocation Solver.

- Geolocation Solver: This service estimates the end devices' position in both networks separately. It uses an LDPL-M algorithm further described in the following sections. This service is implemented using a Python http module. After calculating the end device's position, the coordinates are sent to the NestJS web server via HTTP.
- NestJS Web server: A simple web server storing information about the end devices' location in the database (for each device in both networks separately). This service also contains the ”Where is my node ?” user interface described in section 4.8 in more detail.

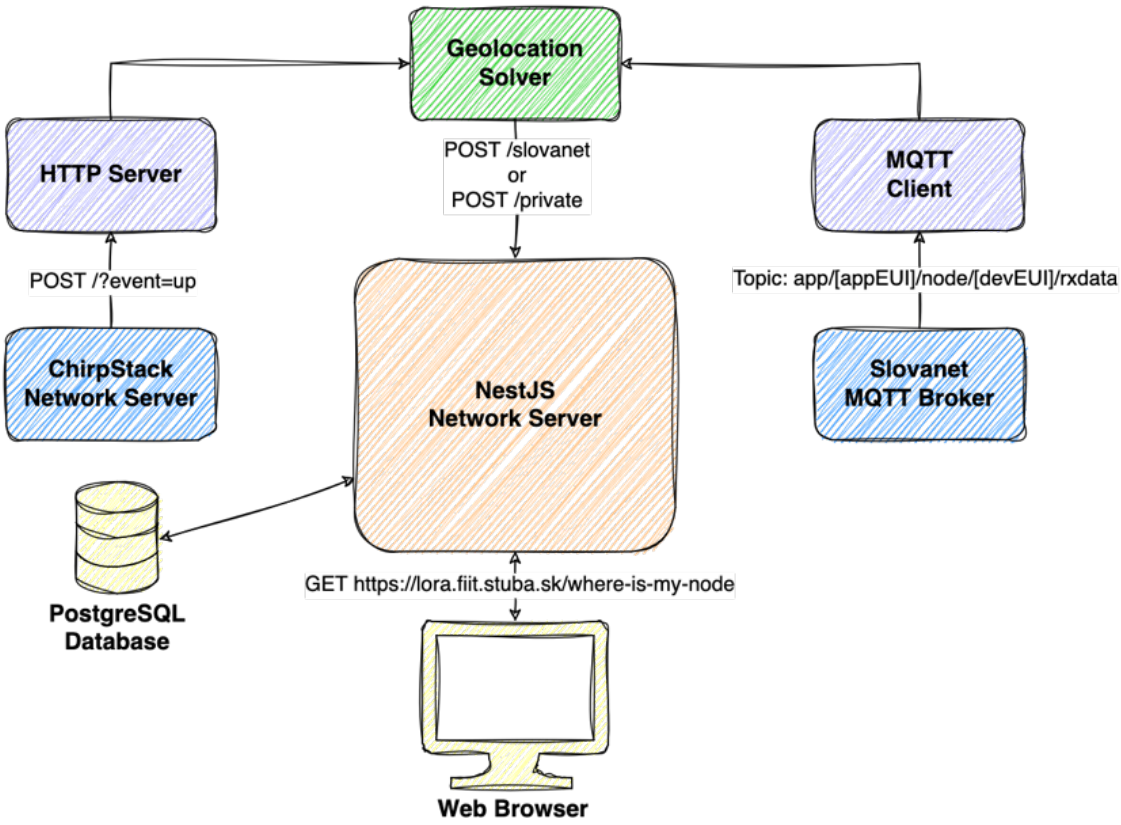

Figure 4 *Software architecture*

3.2 Initial position estimation

Algorithms that determine the location of the end device typically need an initial estimate of the starting position. This accuracy can be slightly lower, as the algorithms should eventually converge to a more accurate results. We used the Weighted Centroid (WC) of the gateways that received the signal from the end device for the initial estimate. The path loss for the given gateway determined the weight. The inspiration for this idea came from a solution proposed by Bissett [20] - weight was linked to the ToA. We assumed that a lower path loss value indicates a gateway closer to the end device and vice versa. Based on this assumption, we calculated the weight for each gateway as follows:

$$w_i = \frac{L_{PL_n} - L_{PL_i}}{L_{PL_n}} + \frac{c}{n}, \tag{9}$$

where: w_i is a weight of ith gateway's influence on the gravity center calculation,

L_{PL_i} is a path loss of the i[th] gateway of the given transmission,
L_{PL_n} is the largest path loss of the given transmission,
c is a constant adding minimum weight for each gateway,
n is a number of gateways that received the uplink message.

The resulting formula for calculating the estimated initial value is as follows:

$$\begin{pmatrix}\hat{x}\\ \hat{y}\end{pmatrix} = \sum_{i=1}^{n} \widehat{w}_i \begin{pmatrix}x_i\\ y_i\end{pmatrix}, \tag{10}$$

where: $\begin{pmatrix}\hat{x}\\ \hat{y}\end{pmatrix}$ is a weighted centroid of gateways' gravity, i.e. estimated starting position of end device.

In addition to estimating the initial position, we used a weighted centroid as one of the techniques to determine the actual position.

3.3 Map projection

Coordinates define the location on the ground. There are two coordinate systems: the Geographic Coordinate System (GCS) and the Projected Coordinate System (PCS). GCS defines the position in angles based on latitude and longitude from the center of the Earth [27]. PCS, or Cartesian Coordinate Systems (CCS), represents the three-dimensional GCS in two dimensions by projecting and leveling the Earth's surface onto a plane. During projection, distortions occur (shape, area, distance, or direction). No kind of projection preserves all four geographic features at the same time. Each projection tries to preserve some geographical feature but with the knowledge of compromising other features. For this reason, many different projections are divided into three main projection systems: cylindrical, conical, and planar. We will focus on the cylindrical projection, as with this type of projection, the lines of latitude and longitude remain parallel to the x and y axes [20, 27].

Figure 5a shows the Mercator projection, one of the most popular and used cylindrical projections. It is used in most map applications such as Google Maps or OpenStreetMap. However, this type of projection distorts areas further from the equator. Another projection type is more suitable for our needs, i.e., the Equidistant projection shown in Figure 5b. It maintains constant distances along both lines of latitude and longitude. In Equidistant projection, we can directly assign the displayed pixel on the map to the corresponding geographic location on Earth.

By a simple calculation, we can convert the GCS to the PCS, i.e., convert the latitude and longitude *(λ, ϕ)* to coordinates *(x, y)* in the Cartesian plane [20, 27, 28]:

$$\begin{aligned} x &= R(\lambda - \lambda_0)\cos\phi_1, \\ y &= R(\phi - \phi_1), \end{aligned} \tag{11}$$

where: x is a horizontal coordinate on projected map,
y is a vertical coordinate on projected map,
R is an Earth radius in meters,
λ is a projected longitude,
λ_0 is a central map parallel,
ϕ is a projected latitude,
ϕ_1 is a standard parallel.

a) **b)**

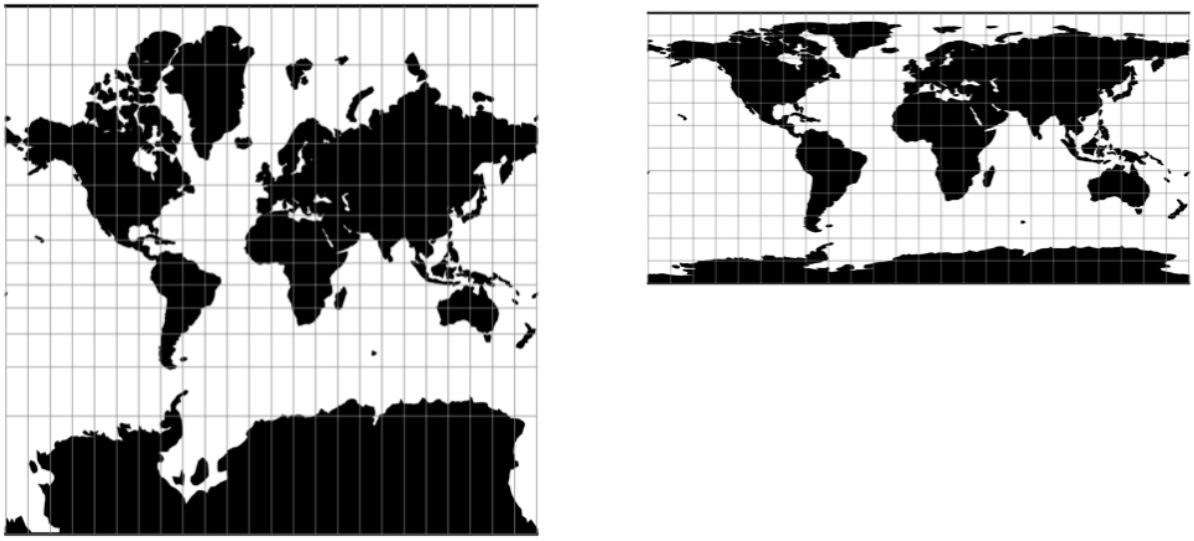

Figure 5 *Cylindrical (a) Mercator and (b) Equidistant projections [28]*

3.4 Accuracy evaluation

The distance between two points must be calculated to evaluate the accuracy or error of the location determined by the techniques described in this article. On a small scale, it can be assumed that the observed surface is flat without the curvature of the Earth. The distance D between the point $P = (\lambda_1, \phi_1)$ and $Q = (\lambda_2, \phi_2)$, can be thus calculated using the simple Euclidean distance [29]:

$$D = R\sqrt{\Delta\phi^2 + (\cos\phi_m \Delta\lambda)^2}, \tag{12}$$

where: R is the radius of the Earth,
$\Delta\phi$ $|\phi_2 - \phi_1|$,
$\Delta\lambda$ $|\lambda_2 - \lambda_1|$,
ϕ_m $\frac{\phi_1+\phi_2}{2}$.

Euclidean distance only approximates the distance between two geographic points if they are relatively close to each other. Since the Earth is not flat, we must calculate the so-called great-circle distance. We can imagine this distance as the length of the shortest rope laid on the Earth surface, which connects two points, as shown in Figure 6 [29]:

$$D = R\tan^{-1}\left(\frac{\sqrt{(\cos\phi_2 \sin\Delta\lambda)^2+(\cos\phi_1 \sin\phi_2-\sin\phi_1 \cos\phi_2 \cos\Delta\lambda)^2}}{\sin\phi_1 \sin\phi_2+\cos\phi_2 \cos\phi_2 \cos\Delta\lambda}\right). \tag{13}$$

Using this technique, we assume that the Earth is a perfect sphere. However, the Earth is an irregular ellipsoid. When calculating the distance between two points, the error is never more significant than 0.5% [30]. Using (13), it is possible to calculate the distance between two points and thus verify the error rate of the geolocation methods.

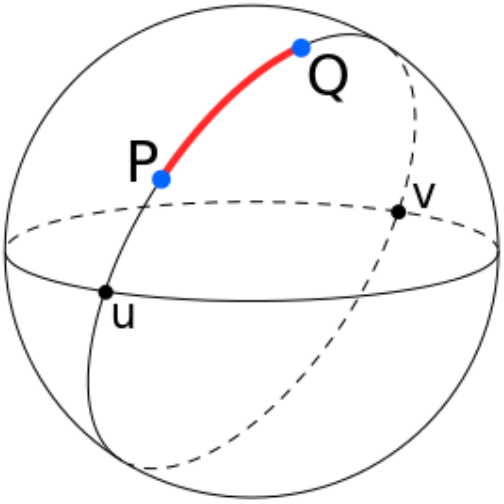

Figure 6 *Great-circle distance [29]*

3.5 Methodology of data collection and processing

Slovanet provided us an end device from the manufacturer Ursalink, which periodically communicated with gateways connected to the public provider LoRaWAN network. In the private LoRaWAN network, we used the end device described in Section 3.1. The process of data collection was similar in both networks. To accurately record the real-time position of the end device, we utilized an external ublox GPS sensor with a precision of 1.5 cm. This sensor was placed next to end devices during measurements, and the position was recorded twice per second. The GPS sensor was also utilized to position the gateways. It is worth noting that the coordinates of the end device were processed not at the time of transmission but at the time of reception at the network server. The processing of measured data consisted of several steps:

1. Assignment of the recorded position by external GPS sensor to uplink messages based on timestamps.
2. Transformation of latitude and longitude into x and y coordinates using local cylindrical equidistant projection.
3. Determination of parameter values ($L_{PL}(d0)$ and β) for individual gateways.
4. Evaluation of the accuracy of geolocation.

The data collected from both networks are visualized in Figure 7a and Figure 7b.

The first step was to assign the location of the end device to uplink messages based on the timestamps. Since the external GPS sensor recorded its position twice per second, it often happened that the time of uplink message reception at the network server was not precisely the same as that of the external GPS sensor. In such a case, the location was selected at the time closest to the message reception time. The difference never exceeded 500 ms.

The second step consisted of transforming latitude and longitude coordinates into x *and* y coordinates using a local cylindrical equidistant projection. To transform the coordinates while preserving the actual scale, it was first necessary to determine ϕ_1 *and* λ_0. To verify the correctness of the so-called true scale equidistant cylindrical projection, we compared the distance between the two most distant points in the dataset using the Euclidean distance in the Cartesian two-dimensional plane and the great-circle distance. The maximum possible distance error between two points using the Euclidean distance versus the great-circle distance was 0.000019 mm (0.0000000084 %) at a length of 228.77 m.

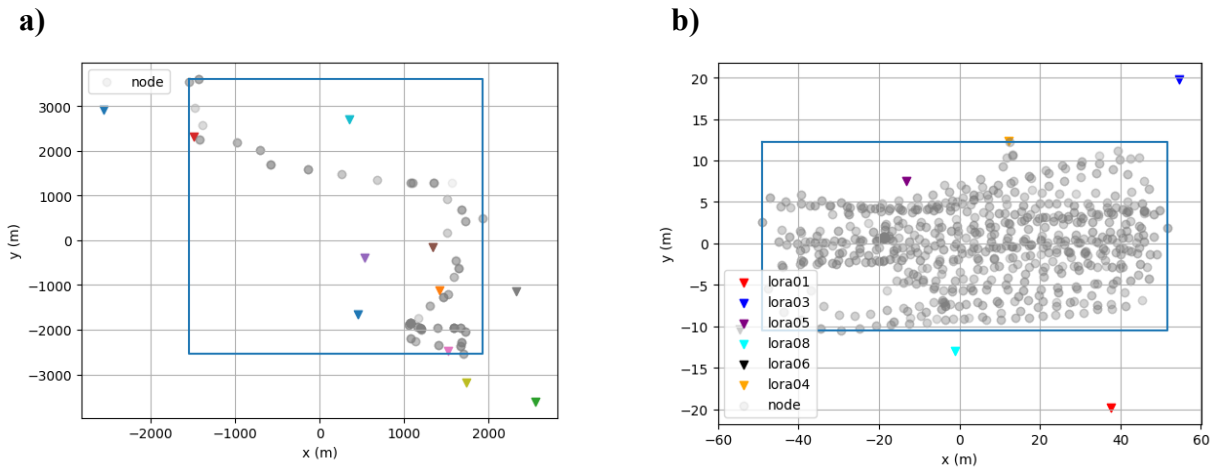

Figure 7 *Visualization of measured data in (a) public provider and (b) private network using equidistant cylindrical projection*

The margin of error is small enough that we can continue to work with the x and y coordinates in the Cartesian plane and use the Euclidean distance.

The next step was determining the values of the parameters ($L_{PL}(d0)$ and β) for individual gateways laying the logarithmic curve so that it best describes the relationship between distance and path loss. We can observe the theoretical FSPL model, compared to the LDPL model, is highly underestimated and unsuitable for determining the location of the end device. Based on the results, we conclude that even a tiny obstacle between the gateway and the end device results in large fluctuations in the path loss, thus significantly affecting the geolocation accuracy. After obtaining the gateway parameters, we calculated the distance of the end device from the gateway using the path loss.

The penultimate step was to perform filtering of uplink messages unsuitable for determining the location of the end device. After filtering out these messages, 132 of the original 233 messages could be used to determine the location of the end device.

The last step was to evaluate the accuracy of geolocation techniques.

3.6 LDPL-M Model

To determine the location of the end device, we propose to use the trilateration method, i.e. to associate the distance of the device from individual gateways based on the value of signal loss during propagation. The reason for using this method is the insufficient time synchronization between the gateways caused by hardware limitations. This fact does not allow us to determine the position of the device using the multilateration method.

The collected dataset has a characteristic feature - since the end device sends uplink messages regularly in a certain period, we can use this fact and potentially improve the overall geolocation accuracy by incorporating the previous locations into the calculation. The condition for this approach is to have the real location of the end device at the time of sending the first message. We can obtain this data either by one of the methods for determining the location or by using the real location using GPS. In addition to the location of the device at the time of sending the first message, it is necessary to determine a value that represents how far the device will most likely move until the next message reception. We can determine the distance that the device can potentially travel in two ways:

1. Calculate all distances between individual transmissions of uplink messages based on empirical measurements and then determine the largest distance that the device

has traveled in 90% of cases. Depending on the use case, this percentage can be adjusted as needed.

2. Determine how fast the device most often moves and thus associate the distance traveled with the device's speed and the periodicity of the uplink message transmission.

After defining the distance that the device will most likely travel between individual transmissions, we propose to use the previous location of the device as the location of an additional virtual gateway in the next transmission. The location of this virtual gateway will represent the center of a circle with a radius equal to the defined distance that the device will most likely travel. By adding the virtual gateway, we can potentially improve the geolocation of the end device using the trilateration method, since we virtually increase the number of gateways that have captured the message. The limitation of this method lies in the assumption that the device moves constantly, or its speed is part of movement data, i.e. known in advance or are a part of the data payload, respectively.

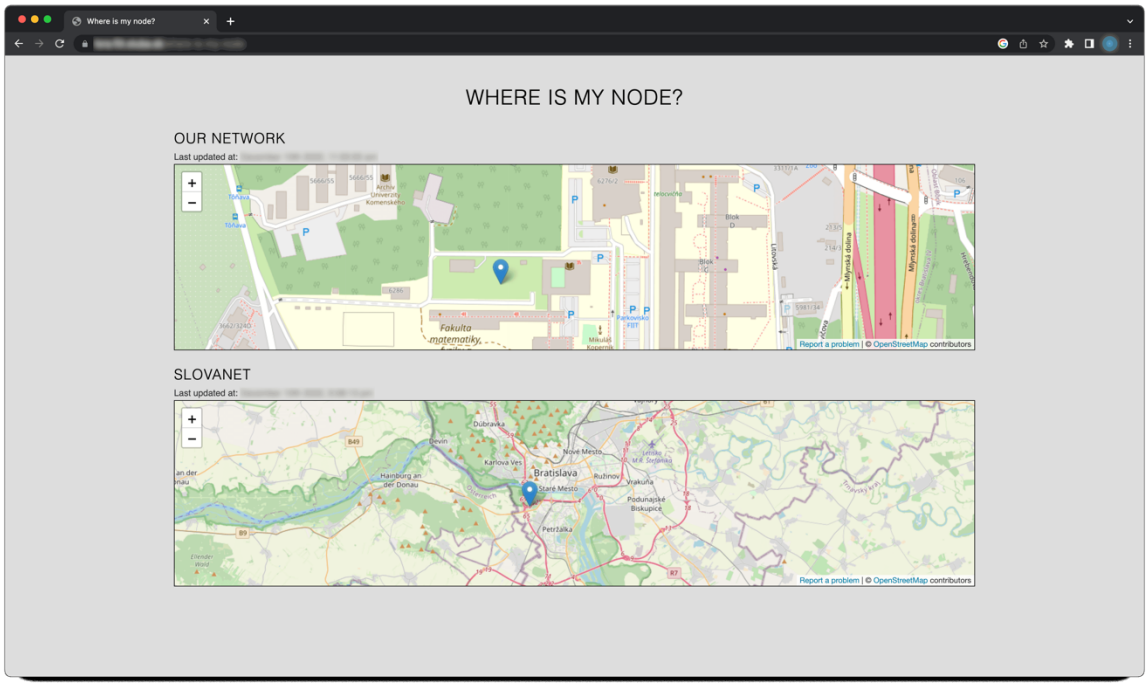

Figure 8 *User interface*

In the case of a static device, the algorithm would worsen the measured results, since it assumes the device is in motion. Furthermore, this algorithm is not suitable for use cases where the speed of the end device slows down or speeds up significantly. We thus in this article propose a novel LDPL-M algorithm and experimentally verify the accuracy of the geolocation on real data and compare the accuracy with the common trilateration methods described in previous sections.

In the previous geolocation techniques, we assumed that the end device was in motion. However, in real-world scenarios, we often encounter situations where end devices are stationary. In the context of computing the end devices' location within the LoRaWAN network, we were able to leverage this observation to enhance the accuracy of our model. To do this, we gathered a set of messages from the private LoRaWAN network, all gathered close to each other (within a 2-meter range). By doing this, we effectively created a scenario mimicking a stationary device. In determining the stationary end device’s location, we incorporated the

current estimation and the results of past calculations. This was achieved by averaging the current estimated location with the results obtained from prior computations. To ensure stability and mitigate significant variations in the RSSI due to environmental factors, we limited the averaging process to the last *N* previously estimated end device's locations. This approach averages the location estimate to smooth abrupt RSSI value changes, potentially refining the geolocation accuracy for stationary end devices. It is important to note that two different methods of averaging location exist:

1. The first way is to figure out the current location and then find the average of the locations determined before.
2. The second way is to figure out the current location and then find the average of earlier locations that had already been threatened the same way (averaged).

The second method provided better results for our use cases.

3.7 "Where is my node ?"

The web application visualizing the location of the end device is called ”Where is my node ?”. It is fully containerized using the Docker platform. A location update occurs every time an uplink message is received from the end device. The user interface is shown in Figure 8. It displays the timestamp of the last location update. The page overviews the geolocation from both the public provider and private LoRaWAN networks.

4 Dataset

During the measurements, a dataset from the private and the Slovanet public provider network was created. We used the ublox external GPS sensor to gather the precise location data, shown in Figure 9c, as a reference. The format of messages received in the public provider network slightly differs from those captured in a private network. Therefore, it was necessary to reflect this fact during implementation of the custom parser, which combines geographical data from an external GPS sensor and uplink message based on the timestamps. The dataset is publicly available for the community at the link *https://data.ail.sk/dataset-geolora/*.

In private network we utilized a LilyGo TTGO ESP32 end device equipped with an SX1276 LoRa chip and built-in NEO-6M GPS module. The end device is shown in Figure 9a. The external GPS sensor near the end device serves as a ground truth for the proposed solution verification. When the end device sent an uplink message, it was processed by the ChirpStack network server, which supports the integration functionality and enables uplink messages to be forwarded in JSON format to external HTTP server and further processed. The server then extracted the message reception timestamp from the message and appended a new line to the Comma-Separated Values (CSV) file. The output file was then combined with the GPS sensor data using a custom parser. Finally, the static information about the location of individual gateways was added.

In public provider network, we utilized end device from the manufacturer Ursalink, shown in Fig. 9b. Access to the data was possible when receiving the message or by obtaining historical data stored in the cache. The cache stores messages for 30 days and can be downloaded via the Representational State Transfer Application Programming Interface (REST API) in JSON format at most once a day. On the other hand, the MQTT protocol allows the subscription to the topic of interest and thus provides access during packet reception. We collected data using the MQTT client. The uplink messages were being sent with 5-minute periodicity. This attribute was set by the provider and could not be further modified.

The only difference worth noting, compared to private network, was encountered when filtering messages unsuitable for geolocation. The location of the gateways in the public provider network was contained within packet data, as we did not have access to the physical

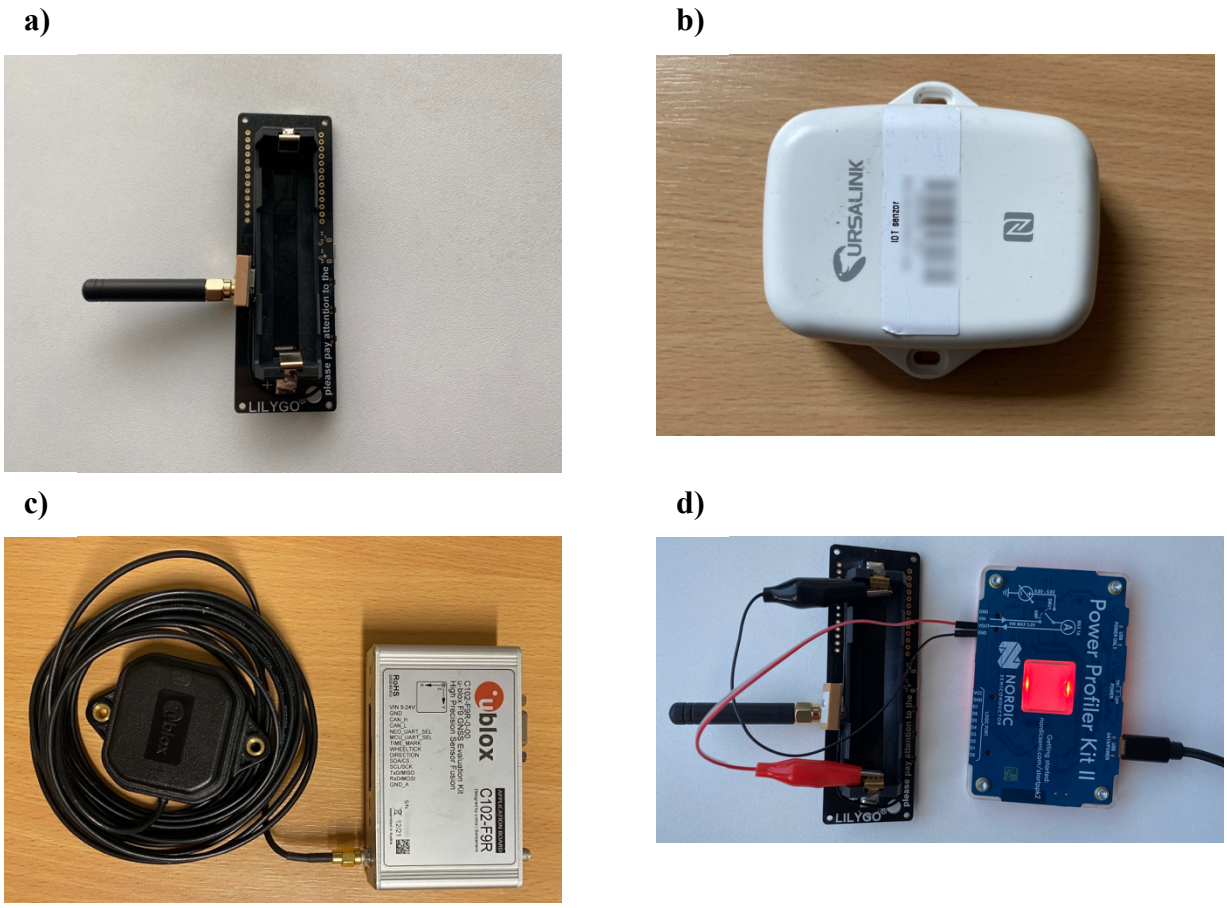

Figure 9 *Hardware used during experimental setup - (a) LilyGo TTGO end device, (b) Ursalink end device, (c) ublox GPS sensor and (d) Power profiler kit II connected to the end device*

topology. However, not every gateway had information regarding its location available. Therefore, it was necessary to remove such gateways from the uplink data and then evaluate whether the appropriate message was received by at least three gateways whose location was known to be able to apply the trilateration-based mechanism.

5 Results and discussion

When determining the location of end devices, we compared techniques discussed in this article - FSPL, LDPL, WC, and our proposed, LDPL-M. The precision of individual techniques was also compared to the GPS sensor data. In all cases working with path loss, we substituted RSSI with ESP.

The results of the error rate in the private LoRaWAN network with DLoS can be seen in Figure 10 showing a plot of the CDF, detailed in Table 1. These results clearly show that the most accurate way to determine the location of the end device is to use a GPS sensor, which is located directly on the top of the device itself but at the expense of increased power consumption. A similar average error is observed for all discussed techniques. However, the difference in accuracy between the LDPL model with and without memory is more significant. Our proposed LDPL-M method improves the geolocation accuracy over the conventional LDPL model by 24.54 % in 90 % of cases. WC results in a similar accuracy, but this method is only applicable for determining the location within the polygon formed by the gateways. The disadvantage is that the nature of the device must be known in advance, i.e., the speed at which the device moves. This limits the possibilities of using the technique. However, the end device

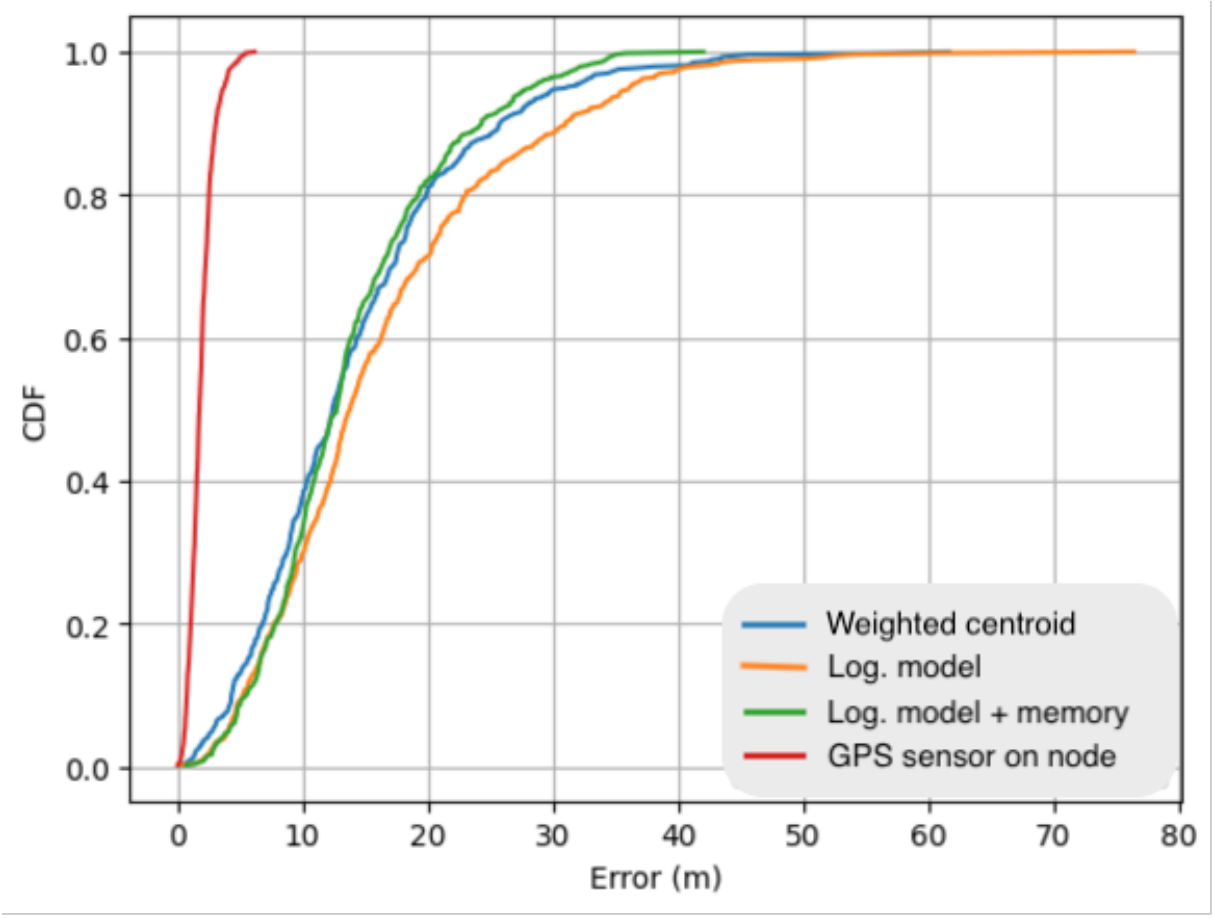

Figure 10 *Accuracy comparison in private network*

can also send the measured or estimated speed inside the LoRaWAN packet payload.

The detailed error results for the public provider LoRaWAN network without DLoS can be seen in Figure 11 and Table 2. During this test, we walked around Bratislava with the device attached rather than staying in the reserved area defined by spread gateways. The results show that the absence of DLoS and densely built regions significantly impacted the geolocation accuracy. Relying solely on RSSI values for estimating location in LoRaWAN networks without DLoS is unreliable. While our proposed model has improved the overall

Table 1 *Error rate comparison in private network (DLoS)*

Method	*90 percentile error (m)*	*50 percentile error (m)*
GPS Sensor	3.11	1.78
LDPL-M	24.33	12.76
WC	25.80	12.43
LDPL	31.01	13.83

accuracy of determining the location of the end device, the error rate is still high for most use cases.

Substituting the RSSI with ESP had a significant impact on the geolocation accuracy in the public provider network. In 90% of cases, the error rate using the RSSI value to calculate the path loss in the LDPL model was less than or equal to 2478.31 m, while using the ESP value it was 2197.53 m. We therefore observe a significant improvement in determining the location (11.35%). The impact of using the ESP decreases if the device is located closer to the gateway

or with DLoS, because ESP partially considers the influence of the environment on the final RSSI.

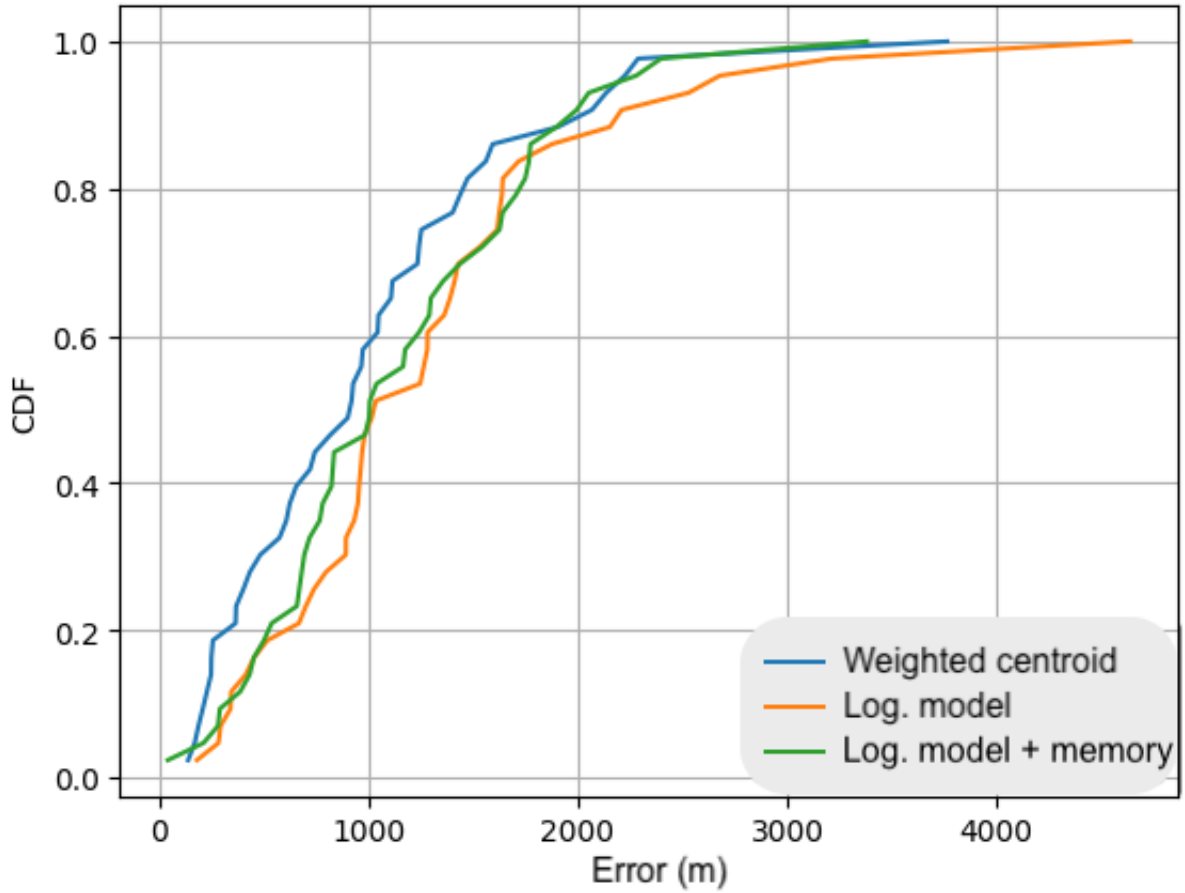

Figure 11 *Accuracy comparison in public provider network*

In the case of an environment with DLoS, the ESP differs minimally from RSSI, which we could observe in the data collected in private network. However, it is still advisable to use the ESP value instead of RSSI.

Table 2 *Error rate comparison in public provider network (no DLoS)*

Method	*90 percentile error (m)*	*50 percentile error (m)*
LDPL-M	1974.99	1006.42
WC	2034.64	919.51
LDPL	2197.53	1035

Regarding the modification proposed for static end devices, Table 3 and Table 4 contain the comparison of error rate between the original and modified geolocation techniques for the static end device. The graphs of CDF curves for individual measurements are present in Figure 12a and Figure 12b.

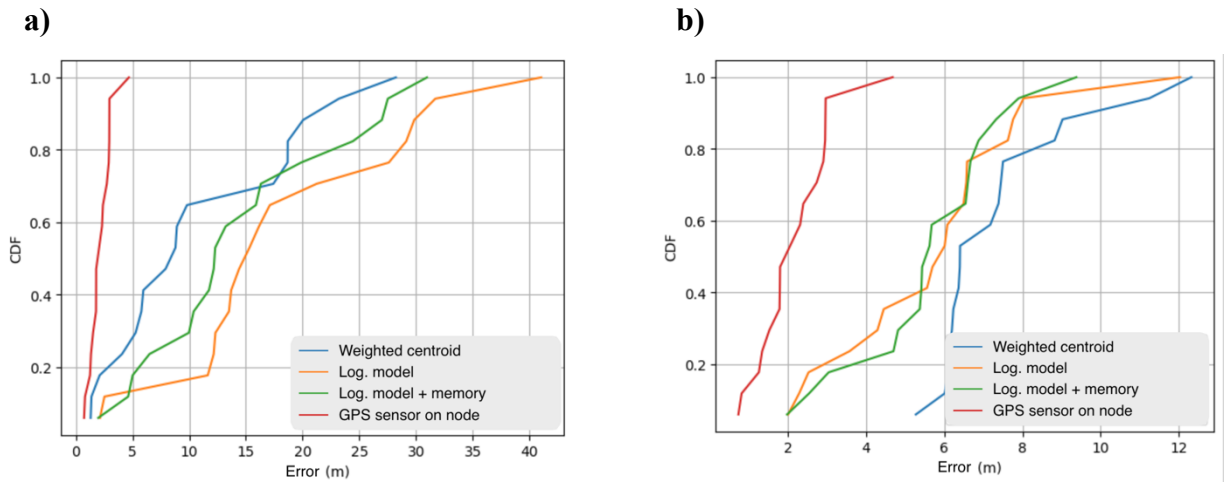

Figure 12 *Accuracy comparison of (a) original and (b) modified methods for static node*

The outcomes indicate that the modified methods enhance geolocation accuracy. We incorporated the results of the previous $N = 10$ calculated locations when averaging.

Table 3 *Error rate for static node using original methods in private network*

Method	*90 percentile error (m)*	*50 percentile error (m)*
LDPL-M	27.20	12.29
WC	21.31	8.79
LDPL	30.59	15.31

The precision of our proposed LDPL-M algorithm increased from the initial 27.20 m to 7.56 m in 90 % of cases. Thus, it is evident that determining the location of a stationary end device is significantly more accurate than determining the position of a moving device.

Table 4 *Error rate for static node using original methods in private network*

Method	*90 percentile error (m)*	*50 percentile error (m)*
LDPL-M	7.56	5.62
WC	9.92	6.40
LDPL	7.87	6.01

Our study also compared energy consumption between scenarios with and without an active GPS module during message transmission and reception. To measure power consumption, we utilized the Power Profiler Kit II from Nordic Semiconductor [30], connected in sequence with the end device's battery pins, as shown in Fig. 9d. Bundled software recorded fluctuations in current over time.

Table 5 *GPS module power consumption measurements*

GPS module	*Average (mA)*	*Transmission (mA)*	*RX window opened (mA)*
Off	86	140	102
On	128	165	141

The results are detailed in Table 5. The measurements showed that the end device power consumption significantly increased (by an average of 48.8 %) when the GPS module was active. This finding underscores that utilizing the GPS module for determining end device's location yields notably enhanced accuracy compared to the trilateration technique used in the LoRaWAN network. However, this advantage comes at the expense of a significantly higher power consumption.

6 Conclusion

Geolocation of the end device in LPWANs while maintaining low power consumption over a relatively large area is an exciting area that opens up many use cases. Choosing the proper technique to determine the location in the LoRaWAN network requires a thorough evaluation of advantages and disadvantages, especially in terms of overall efficiency.

In our article, we focused on comparing existing techniques using the private LoRaWAN network as well as the public provider LoRaWAN network provided by Slovanet. Next, we described the process of collecting and processing data. We proposed a novel LDPL-M algorithm to enhance the geolocation accuracy concerning low power consumption. Compared to existing techniques, the LDPL-M also considers the end device's previous locations. To assess the accuracy, we determined the location of the end device using an external GPS sensor and matched collected uplink messages with GPS sensor data. Part of our work was dedicated to estimating the end device's starting position as an input to discussed geolocation methods. We observed a significant environmental influence on the RSSI value. Our measurements confirmed that the geolocation of end devices in the LoRa network by the trilateration is possible; however, it is not suitable for densely built-up areas and without DLoS. During experiments, the LDPL-M achieved better results than commonly used techniques. We assessed the impact of the GPS module on the end device's power consumption. Results revealed a notable increase with GPS enabled (average rise of 48.8%). This result indicates that using a GPS module is significantly more accurate than the trilateration technique in LPWANs, but at the cost of higher power consumption. At the same time, we observed a significantly lower error rate for determining the location of a static end device compared to a device in motion. Finally, we implemented a web application that displays the location of the end device in real time in both the private and public provider networks.

To our knowledge, we have yet to find any similar dataset that pairs geographic data with uplink reports from Bratislava, Slovakia. Our study provides measured data to the community for future research. Our measurements confirm that the environment significantly affects the RSSI. As a part of our research, we proved that the proposed LDPL-M algorithm achieves better results than commonly used techniques under specific conditions.

The subject of future work could be developing the geolocation method based on the multilateration using the TDoA principle. This method requires modifying the gateway hardware, which must be equipped with a GPS module to ensure a high degree of time synchronization between individual gateways. It would be necessary to collect data further and compare the accuracy of the TDoA method with the trilateration method based on the RSSI used in this work.

Acknowledgements

Funded by the EU NextGenerationEU through the Recovery and Resilience Plan for Slovakia under the project No. 09I05-03-V02-00012. This project has been supported by APVV-23-0137 project "Legal and technical aspects of cybersecurity situational awareness". The authors would like to thank for financial contribution from the STU Grant scheme for Support of Young Researchers. The authors would also like to express their gratitude to Slovanet, a.s. for granting access to the public provider network and borrowing the equipment necessary for the research.

Conflicts of interest

The authors declare that they have no known competing financial interests or personal relationships that could have appeared to influence the work reported in this article.

References

[1] SINHA, R., YIQIAO W., HWANG, S. A survey on LPWA technology: LoRa and NB-IoT. ICT Express [online]. Science Direct. 2017, 3(1), p. 14–21 [accessed 2025-04-15]. ISSN 2405-9595. Available from: https://doi.org/10.1016/j.icte.2017.03.004

[2] LINK LABS A Comprehensive Look at Low Power, Wide Area Networks [online]. 2016 [accessed 2025-04-15]. Available from: https://www.link-labs.com/low-power-wide-area-networks-white-paper

[3] GARCHE, J., DYER, C. Encyclopedia of Electrochemical Power Sources. Elsevier, 2009. ISBN 9780444520944.

[4] CHENEBAULT et al. Impedance analysis of the lithium discharge in Li-$SOCl_2$ cells: Synergetic effect of SO_2 and $LiAl(SO_3Cl)_4$ [online]. Journal of Applied Electrochemistry. 1989, 19(3), p. 413-420 [accessed 2025-04-15]. Available from: https://doi.org/10.1007/BF01015245

[5] ANJUM, M. et al. Analysis of RSSI Fingerprinting in LoRa Networks. In: 2019 15th International Wireless Communications & Mobile Computing Conference (IWCMC). Tangier, Morocco, 2019. ISBN 978-1-5386-7748-3, p. 1178-1183.

[6] ARAS, E. et al. Exploring the Security Vulnerabilities of LoRa. In: 2017 3rd IEEE International Conference on Cybernetics (CYBCONF). Exeter, UK, 2017. ISBN 978-1-5386-2201-8, p. 1-6.

[7] LORA ALLIANCE LoRaWAN Specification v1.1 [online]. 2017 [accessed 2025-04-15]. Available from: https://lora-alliance.org/resource_hub/lorawan-specification-v1-1/

[8] SEMTECH CORPORATION LoRa and LoRaWAN [online]. 2024 [accessed 2025-04-15]. Available from: https://www.semtech.com/uploads/technology/LoRa/lora-and-lorawan.pdf

[9] PERESINI, O., KRAJCOVIC, T. More efficient IoT communication through LoRa network with LoRa@FIIT and STIOT protocols. In: 2017 IEEE 11th International Conference on Application of Information and Communication Technologies (AICT). Moscow, Russia. 2017. ISBN 978-1-5386-0502-8, p. 1-6.

[10] MONTAGNY, S. LoRa - LoRaWAN and Internet of Things for beginners [online]. Université Savoie Mont Blanc, 2021 [accessed 2025-04-15]. Available from: https://www.univ-smb.fr/lorawan/wp-content/uploads/2022/01/Book-LoRa-LoRaWAN-and-Internet-of-Things.pdf

[11] PODEVIJN, N. Experimental TDoA localisation in real public LoRa networks. In: Short Paper Proceedings of the Tenth International Conference on Indoor Positioning and Indoor Navigation - Work-in-Progress Papers (IPIN-WiP 2019) co-located with the Tenth International Conference on Indoor Positioning and Indoor Navigation (IPIN 2019) [online]. Pisa, Italy. 2019 [accessed 2025-04-15]. p. 211-218. Available from: https://ceur-ws.org/Vol-2498/short28.pdf

[12] FARGAS, B., PETERSEN, M. GPS-free geolocation using LoRa in low-power WANs. In: 2017 Global Internet of Things Summit (GIoTS). Geneva, Switzerland. 2017. ISBN 978-1-5090-5874-7, p. 1-6.

[13] ZUCCONI, A. Positioning and Trilateration [online]. 2017 [accessed 2025-04-15]. Available from: https://www.alanzucconi.com/2017/03/13/positioning-and-trilateration/

[14] OGUEJIOFOR, O. et al. Trilateration Based Localization Algorithm for Wireless Sensor Network. International Journal of Innovative Science and Modern Engineering (IJISME) [online]. 2013. 1(10). p. 21-27 [accessed 2025-04-15]. ISSN 2319-6386. Available from: https://www.ijisme.org/wp-content/uploads/papers/v1i10/J04470911013.pdf

[15] Dawoud, S. GNSS principles and comparison [online]. Potsdam University. Potsdam, Germany. 2012 [accessed 2025-04-15]. Available from: http://www.snet.tu-berlin.de/fileadmin/fg220/courses/WS1112/snetproject/gnss-principles-and-comparison_dawoud.pdf
[16] LESTABLE, T., LALAM, M., GRAU, M. Location-Enabled LoRa IoT Network: Geo-LoRa-ting your assets [online]. 2015 [accessed 2025-04-15]. Available from: https://www.slideshare.net/slideshow/io-t-sagemcom-m2minnovationworldgeotrackv08/52922413
[17] RUSLI, M. et al. An Improved Indoor Positioning Algorithm Based on RSSI-Trilateration Technique for Internet of Things (IOT). In: 2016 International Conference on Computer and Communication Engineering (ICCCE). Kuala Lumpur, Malaysia. 2016. ISBN 978-1-5090-2428-5, p. 72-77.
[18] YANG, Z., LIU, Y. Quality of Trilateration: Confidence Based Iterative Localization. In: 2008 The 28th International Conference on Distributed Computing Systems [online]. Beijing, China. 2008. ISSN 1063-6927, p. 446-453. Available from: https://doi.org/10.1109/ICDCS.2008.59
[19] SEMTECH CORPORATION AN1200.22 LoRa Modulation Basics [online]. 2015 [accessed 2025-04-15]. Available from: https://www.frugalprototype.com/wp-content/uploads/2016/08/an1200.22.pdf
[20] BISSET, D. Analysing TDoA Localisation in LoRa Networks. Master's thesis [online]. Delft: TU Delft, Faculty of Electrical Engineering, Mathematics and Computer Science. 2018 [accessed 2025-04-15]. Available from: https://resolver.tudelft.nl/uuid:bea423b1-6f04-4708-8ed4-e8663dd51cde
[21] GARG, V. Wireless Communications & Networking. San Francisco, CA: Morgan Kaufmann Publishers, Inc. 2010. ISBN 9780080549071
[22] JÖRKE, P. et al. Urban channel models for smart city IoT-networks based on empirical measurements of LoRa-links at 433 and 868 MHz. In: 2017 IEEE 28th Annual International Symposium on Personal, Indoor, and Mobile Radio Communications (PIMRC). Montreal, QC, Canada. 2017. ISBN 978-1-5386-3532-2, p. 1-6.
[23] VALACH, A., MACKO, D. Exploration of the LoRa Technology Utilization Possibilities in Healthcare IoT Devices. In: 2018 16th International Conference on Emerging eLearning Technologies and Applications (ICETA). Stary Smokovec, Slovakia. 2018. ISBN 978-1-5386-7915-9, p. 623-628.
[24] RAHMADHANI, A. Performance Evaluation of LoRaWAN: From Small-Scale to Large-Scale Network. Master's thesis [online]. Delft: TU Delft, Faculty of Electrical Engineering, Mathematics and Computer Science. 2017 [accessed 2025-04-15]. Available from: https://resolver.tudelft.nl/uuid:b8acf9d3-9629-4439-9148-9e66aecbec1c
[25] PARENTE, L. LMIC-node - GitHub [online]. 2021 [accessed 2025-04-15]. Available from: https://github.com/lnlp/LMIC-node
[26] BROCAAR, O. ChirpStack, open-source LoRaWAN Network Server [online]. 2016 [accessed 2025-04-15]. Available from: https://www.chirpstack.io/
[27] SNYDER, J. Map projections: A working manual. Professional Paper 1395 [online]. 1987 [accessed 2025-04-15]. Available from: https://doi.org/10.3133/pp1395
[28] PROJ CONTRIBUTORS PROJ coordinate transformation software library - Open Source Geospatial Foundation [online]. 2025 [accessed 2025-04-15]. Available from: https://doi.org/10.5281/zenodo.5884394
[29] ZUCCONI, A. Understanding Geographical Coordinates [online]. 2017 [accessed 2025-04-15]. Available from: https://www.alanzucconi.com/2017/03/13/understanding-geographical-coordinates/

[30] NORDIC SEMICONDUCTOR Power Profiler Kit II [online]. 2024 [accessed 2025-04-15]. Available from: https://www.nordicsemi.com/Products/Development-hardware/Power-Profiler-Kit-2